Sensitive and selective detection of free FXIII activation peptide: a potential marker of acute thrombotic events

Elisabeth Ortner,[1] Verena Schroeder,[1] Reto Walser,[2] Oliver Zerbe,[2] and Hans P. Kohler[1,3]

[1]Department of Hematology, Hemostasis Research Laboratory, University Hospital Bern, Inselspital, Bern; [2]Institute of Organic Chemistry, University of Zurich, Zurich; and [3]Department of Internal Medicine, Spital Netz Bern Hospitals, Ziegler Tiefenau, Bern, Switzerland

Coagulation factor XIII (FXIII) stabilizes fibrin fibers and is therefore a major player in the maintenance of hemostasis. FXIII is activated by thrombin resulting in cleavage and release of the FXIII activation peptide (AP-FXIII). The objective of this study was to characterize the released AP-FXIII and determine specific features that may be used for its specific detection. We analyzed the structure of bound AP-FXIII within the FXIII A-subunit and interactions of AP-FXIII by hydrogen bonds with both FXIII A-subunit monomers. We optimized our previously developed AP-FXIII ELISA by using 2 monoclonal antibodies. We determined high binding affinities between the antibodies and free AP-FXIII and demonstrated specific binding by epitope mapping analyses with surface plasmon resonance and enzyme-linked immunosorbent assay. Because the structure of free AP-FXIII had been characterized so far by molecular modeling only, we performed structural analysis by nuclear magnetic resonance. Recombinant AP-FXIII was largely flexible both in plasma and water, differing significantly from the rigid structure in the bound state. We suggest that the recognized epitope is either occluded in the noncleaved form or possesses a structure that does not allow binding to the antibodies. On the basis of our findings, we propose AP-FXIII as a possible new marker for acute thrombotic events. (*Blood*. 2010;115(24):5089-5096)

Introduction

Blood coagulation is a highly regulated process and plays a major role in hemostasis. Upon vessel injury, a concerted action of platelets and plasmatic coagulation stop bleeding and trigger repair of the damaged vessel. Blood coagulation factor XIII (FXIII) is the last factor to be activated in the coagulation cascade and its active form functions as a transglutaminase, which covalently cross-links fibrin polymers and antifibrinolytic proteins such as α_2-plasmin inhibitor to fibrin.[1] Because of its function to stabilize fibrin clots, FXIII plays a major role in acute thrombotic events such as myocardial infarction, ischemic stroke, deep vein thrombosis, and pulmonary embolism.[2-6]

In plasma the inactive FXIII zymogen consists of 2 catalytic A-subunits and 2 carrier B-subunits forming the FXIII-A_2B_2 tetramer, which is bound to fibrinogen in physiologic conditions. During activation of plasma FXIII, thrombin cleaves off the N-terminal activation peptide (AP-FXIII), which is subsequently released into plasma,[7] and FXIII is thereby converted to FXIII-A'_2B_2. Binding of Ca^{2+} ions induces the dissociation of the A′- and B-subunits, which is enhanced by the presence of fibrin. Finally, the A′-subunits assume their active configuration (FXIII-A*).[1]

The Val34Leu polymorphism within AP-FXIII has been associated with a protective effect against myocardial infarction, deep venous thrombosis, and ischemic stroke. With an allele frequency of approximately 25%, this polymorphism is common in the white population compared with a rather low percentage in the African or Asian population.[1]

Crystal structure analysis of the FXIII-A_2 homodimer suggests that the N-terminal AP-FXIII crosses the FXIII-A_2 homodimer interface and occludes the catalytic cavity, preventing substrate binding to the zymogen.[8] Hence it was postulated that either the release or significant conformational changes of the AP-FXIII are necessary to expose the catalytic site. In contrast, the authors[9] of another crystallographic study of the FXIII A_2-homodimer proposed that AP-FXIII retains its conformation after thrombin cleavage and remains bound to the FXIII A'_2-homodimer in the same position as within the inactive zymogen. More evidence for the release of AP-FXIII came from our previous study,[7] where we detected free AP-FXIII in plasma and serum. We also suggested structural changes of free AP-FXIII compared with the bound state by ab initio modeling and molecular dynamics simulations.

Here, we investigated for the first time the structure of free AP-FXIII by the use of nuclear magnetic resonance (NMR). We demonstrate that free AP-FXIII is much more flexible than in its rigidly bound form. This unique feature allows selective detection of the cleaved peptide. We used 2 mouse monoclonal antibodies raised against synthetic AP-FXIII to optimize the enzyme-linked immunosorbent assay (ELISA) for selective detection of free AP-FXIII. We characterized the interactions between antibodies and AP-FXIII by surface plasmon resonance (SPR). Both antibodies bind to free AP-FXIII with very high affinities, and binding was not significantly influenced by the Val34Leu polymorphism. Furthermore, we identified nonoverlapping binding epitopes for the 2 antibodies and observed no cross-reactivity with the FXIII-A_2B_2 tetramer or other plasma proteins. Finally, NMR analysis of ^{15}N-labeled recombinant AP-FXIII in water and in plasma proved the peptide to be largely unstructured. Taken together, our data demonstrate that AP-FXIII released into plasma can be selectively detected. We propose that this might be used as a new diagnostic marker for acute thrombotic events.

Submitted November 6, 2009; accepted March 30, 2010. Prepublished online as *Blood* First Edition paper, April 7, 2010; DOI 10.1182/blood-2009-11-253062.

The online version of this article contains a data supplement.

The publication costs of this article were defrayed in part by page charge payment. Therefore, and solely to indicate this fact, this article is hereby marked "advertisement" in accordance with 18 USC section 1734.

Methods

Contacts of AP-FXIII within the FXIII A-subunit dimer

The conformation of AP-FXIII when still attached to the FXIII A-subunit was analyzed by use of the coordinates from the 2.1 Å crystal structure,[10] protein database entry 1F13 (http://www.rcsb.org/pdb). Positions of amino acids 1-4 and 37-38 were not resolved in the crystal structure. Visualization of the FXIII A-subunit dimer and analysis of interactions of AP-FXIII residues with surrounding amino acids was performed with the Swiss PDB Viewer,[11] version 4.0.1.

Antibodies and peptides

Mouse monoclonal antibody mAb-6B11 against human AP-FXIII was developed in collaboration with GENOVAC GmbH. For immunization, a synthetic AP-FXIII was generated according to the published sequence (Swiss-Prot entry P00488) with an additional cysteine residue at its N-terminus (CSETSRTAFGGRRAVPPNNSNAAEDDLPTVELQGVVPR) and coupled to the carrier protein keyhole limpet hemocyanin. After immunization and subcloning, the monoclonal antibody (immunoglobulin G_1) was purified by the use of a protein-G affinity column, and its purity was verified by sodium dodecyl sulfate polyacrylamide gel electrophoresis. The production of the mouse monoclonal antibody mAb-1286 raised against human AP-FXIII was previously described.[7] Synthetic peptides corresponding to full-length AP-FXIII with an additional N-terminal Cys and containing either Val or Leu at position 34 (AP-FXIII-Val and AP-FXIII-Leu) were produced by ABGENT Inc. AP-FXIII fragments AP1 to AP9, AP1-12, AP3-12, and AP13-37 were obtained from GenScript Corp.

AP-FXIII ELISA analyses

We optimized the previously published sandwich-type ELISA[7] by using the 2 monoclonal anti-AP-FXIII antibodies mAb-6B11 and mAb-1286 with the latter biotinylated. In brief, 96-well microtiter plates (Maxisorp; Nunc) were coated with 100 μL of mAb-6B11 at 4 μg/mL in coating buffer (50mM sodium carbonate, pH 9.6). AP-FXIII was diluted in dilution buffer (50mM Tris-HCl, 150 mM NaCl, 0.1% bovine serum albumin, 0.01% sodium azide, pH 7.5) and was loaded in a volume of 100 μL per well. The detection antibody mAb-1286 was used at 2 μg/mL in dilution buffer (50mM Tris-HCl, 150mM NaCl, 0.1% bovine serum albumin, pH 7.5), which was followed by incubation with streptavidin conjugated with alkaline-phosphatase (Fluka Chemie GmbH, a Sigma-Aldrich company) at 1 μg/mL in dilution buffer for 1 hour. Plates were developed with *p*-nitrophenyl phosphate (1 mg/mL in 1M diethanolamine containing 0.5mM $MgCl_2$, pH 9.8; Sigma-Aldrich) for exactly 15 minutes. The color-developing reaction was stopped with 4M NaOH, and optical density (OD) was measured on a microplate reader at 405 nm with a reference filter at 550 nm (Anthos HT3; Anthos Labtec Instruments). We tested the ability of the ELISA to detect native AP-FXIII by analyzing serum samples diluted 1:200 in dilution buffer. To test for cross-reactivity with nonactivated FXIII-A_2 we captured purified FXIII-A_2 using a polyclonal antibody and detected with both monoclonals and a polyclonal as positive control.

Determination of binding affinity and epitope mapping with SPR

We used a Biacore X system (Biacore) on the basis of SPR[12] to measure binding affinities between AP-FXIII and the antibodies mAb-6B11 and mAb-1286 and for epitope mapping. In brief, the antibodies were immobilized on the surface of carboxy-methylated dextran sensor chips (CM5; Biacore) through amine coupling. The surface was activated with a 1:1 mixture of *N*-hydroxysuccinimide and 1-ethyl-3-(3-dimethylaminopropyl)-carbodiimide hydrochloride (amine-coupling kit; Biacore). The antibody mAb-6B11 was injected at a concentration of 20 μg/mL and mAb-1286 at 50 μg/mL in 10mM sodium acetate, pH 5.0, at a flow rate of 10 μL/min. The immobilization reaction was stopped with ethanolamine after the signal had increased by 14 000 resonance units (RU) for mAb-6B11 and by 11 000 RU for mAb-1286.

For determination of the binding affinity and for epitope mapping, the peptides were injected at concentrations increasing from 2.5 to 17nM in HBS-EP buffer (0.01M HEPES [*N*-2-hydroxyethylpiperazine-*N*′-2-ethanesulfonic acid], pH 7.4; 0.15M NaCl; 3mM EDTA [ethylenediaminetetraacetic acid]; 0.005% vol/vol surfactant P20) at a flow rate of 10 μL/min. After passage of each peptide, the surface was regenerated by injection of 10 to 20mM NaOH at a flow rate of 10 μL/min. Data were analyzed by the global fitting algorithm of the BIAevaluation 3.0 software package (Biacore).

Epitope mapping analyses by ELISA

Peptides were directly coated onto 96-well DNA-BIND plates (Corning Inc) at a concentration of 40 μg/mL in dilution buffer in a volume of 100 μL per well. After blocking (50mM Tris-HCl, 150mM NaCl, 1% bovine serum albumin, pH 7.5), the plates were incubated with either mAb-6B11 or mAb-1286 at a final concentration of 2 μg/mL in dilution buffer, followed by incubation with a secondary goat anti-mouse alkaline-phosphatase conjugated antibody (1 μg/mL in dilution buffer; Sigma-Aldrich). Detection was carried out as described previously.

To exclude competition between the 2 antibodies, binding of one antibody to AP-FXIII was studied in the presence of the other. ELISA plates were coated with AP-FXIII at concentrations of 0.4 to 137nM and incubated either with biotinylated mAb-1286 at 2 μg/mL only or in a mixture with mAb-6B11 at 1, 2, or 4 μg/mL. Then, the plates were incubated with a secondary goat anti-mouse alkaline-phosphatase conjugated antibody (1 μg/mL). Detection was performed as described previously.

Expression of ^{15}N-Ub-AP-FXIII in *Escherichia coli* for NMR analyses

We expressed ^{15}N-labeled AP-FXIII as a fusion protein with ubiquitin according to the method of Kohno et al.[13] To obtain the AP-FXIII DNA construct, 2 overlapping primers (forward 5′-TCAGAAACTTCCAGGACCGCCTTTGGAGGCAGAAGAGCAGTTCCA CC CAATAACTCTAATGCAGCGGAAGATGAC-3′, reverse 5′-CGCGTCGACTATCAC CGGGGCACCAAGCCCTGAAGCTCCACTGTGGGCAGGTCATCTTCCGCTGCATTAGA-3′), which contained an additional *Sal*I site and 2 stop codons, were amplified by polymerase chain reaction (PCR). This PCR product was used as template in a second PCR reaction to phosphorylate the 5′-end (forward primer 5′-phospho-TCAGAAACTTCCAGGACCG-3′, reverse 5′-CGCGTCGACTATCACCGG-3′). In preparation for cloning into a pUBK19 vector downstream of the ubiquitin sequence, the AP-FXIII DNA construct was digested with *Sal*I (Fermentas). The vector plasmid was linearized by digestion with Mph1103I (Fermentas), and the blunt ends were generated by T4 DNA polymerase (Invitrogen) followed by digestion with *Sal*I. The AP-FXIII DNA construct was ligated with the vector plasmid to generate the pUBK19-AP-FXIII plasmid.

A detailed description of the expression and purification process of AP-FXIII can be found in the supplemental Methods (available on the *Blood* Web site; see the Supplemental Materials link at the top of the online article). In brief, pUBK19-AP-FXIII was transformed into *E coli C41* cells,[14] which were grown on minimal medium by the use of $^{15}NH_4Cl$ as the sole nitrogen source. The ubiquitin-AP-FXIII fusion protein was purified by Ni-NTA chromatography.

AP-FXIII was liberated from its fusion partner through treatment with yeast ubiquitin hydrolase, and the peptide was finally purified by high-performance liquid chromatography. The mass of the purified peptide was verified by electrospray ionization mass spectrometry (data not shown).

Circular dichroism spectroscopy

Circular dichroism spectra were recorded by the use of 50μM peptide solutions in buffer (20mM 2-[*N*-morpholino]ethanesulfonic acid, pH 5.5, or sodium phosphate, pH 7) on a Jasco J-715 spectrometer at room temperature in a quartz cuvette with a 1-cm path length. Spectra were recorded

covering a range from 190 to 250 nm at a scanning rate of 50 nm/min. Data from 15 scans were averaged to obtain the spectra.

NMR spectroscopy

Spectra were recorded with 1mM samples of uniformly ^{15}N-labeled AP-FXIII dissolved in water or plasma at pH 5.5. The proton-nitrogen correlation map was assigned by the use of standard 3D ^{15}N-resolved Total Correlation Spectroscopy and nuclear overhauser enhancement spectroscopy experiments.[15,16] ^{15}N-NOE values were recorded by the use of a ^{1}H-detected version of the ^{15}N{^{1}H}-steady state heteronuclear Overhauser effect experiment.[17] Spectra were processed in TOPSPIN 2.1 (Bruker) and transferred to the XEASY[18] and CARA[19] program packages for data evaluation.

Statistical analysis

Results from replicate experiments were analyzed by descriptive statistics with Microsoft Office Excel 2007. Results are shown as mean and standard deviation. Concentration curves used to characterize the ELISA were drawn in SigmaPlot 10 (Systat Software Inc). Symbols represent mean values, and error bars represent SD.

Results

Structural analysis of AP-FXIII bound to the FXIII A-subunit

AP-FXIII is part of the FXIII A-subunit and consists of the first N-terminal 37 amino acids. X-ray crystallography of zymogen FXIII-A_2 demonstrated that AP-FXIII tightly associates with residues of the FXIII A-subunit.[8] As shown in Figure 1A and B, AP-FXIII is located on the surface of the A-subunit adjacent to the β-sandwich domain. Its N-terminus overlaps with the barrel 1 domain of the other monomer. Figure 1C shows possible interactions with several amino acids of both monomers. We identified 13 hydrogen-bonds (H-bonds) with residues of the same and 4 H-bonds with residues of the other monomer (Figure 1D). The former include Asn17-Arg107, Asn17-Tyr108, Asn17-Leu249, Asn18-Arg252, Asn20-Lys156, Ala21-Asp243, Glu23-Arg174 (2 H-bonds), Asp24-Arg158, Pro27-Arg171, Thr28-Arg171, Glu30-Val169, and Gln32-Tyr167. The latter include Gly10-Thr561, Arg11-Asp343 (2 H-bonds), and Arg11-Pro399. In addition,

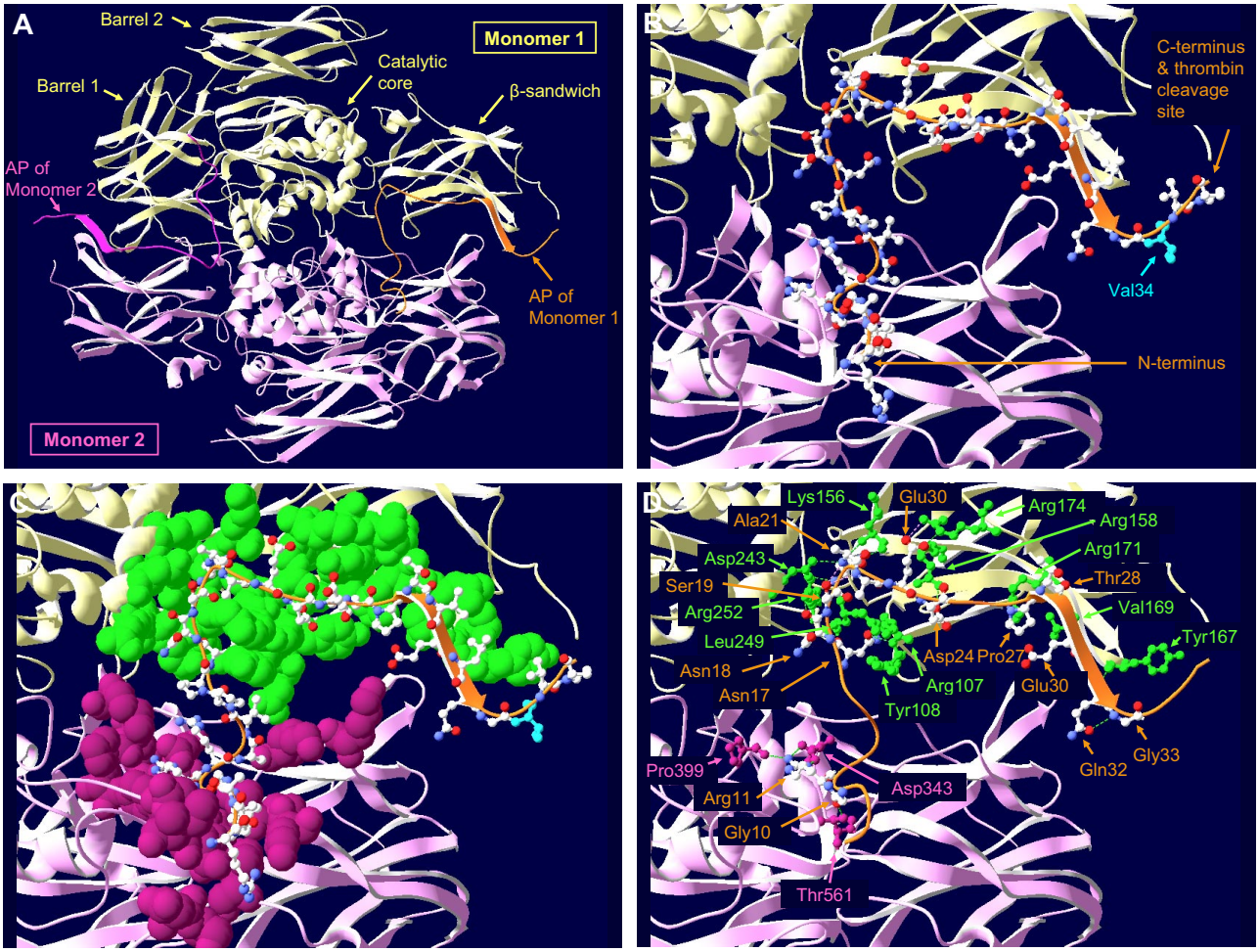

Figure 1. Localization, molecular structure, and interactions of the AP-FXIII within the FXIII A-subunit dimer. (A) Overview of the FXIII A-subunit dimer. The 2 monomers are shown in yellow and pink with their respective AP-FXIII highlighted in orange and dark pink. (B) Detailed picture of the AP-FXIII of monomer 1. The peptide backbone is shown as an orange ribbon with carbon, nitrogen, and oxygen atoms colored in white, blue, and red, respectively. The position of Val34 of the common Val34Leu polymorphism is indicated in light blue. At the N-terminus of the AP-FXIII, amino acids 1-4 are missing, and the gap at the C-terminus represents the missing amino acids 37 and 38. (C) Immediate molecular environment of the AP-FXIII. All amino acid residues on monomer 1 (green space-filled atoms) and on monomer 2 (pink space-filled atoms) that lie within 5 Å from the amino acid residues of the AP-FXIII (ball-and-stick atoms) are shown. (D) H-bonds between amino acid residues of the AP-FXIII and surrounding amino acid residues are shown as dashed lines. H-bonds are drawn if the distance between H-donor and H-acceptor atoms is less than 3.2 Å. Only amino acid residues forming H-bonds are displayed. Amino acid residues of the AP-FXIII are labeled in orange, the residues of monomers 1 and 2 are labeled in green and pink, respectively.

3 H-bonds are formed within AP-FXIII: Ser19-Ala21, Ser19-Ala22, and Gln32-Gly33.

Characterization of the optimized ELISA for free AP-FXIII

We optimized our AP-FXIII–specific ELISA[7] by using the mouse monoclonal antibodies mAb-6B11 and mAb-1286 for capture and detection, respectively. In a first step, we demonstrated that the optimized ELISA measures AP-FXIII over a concentration range between 0.5 and 0.05 ng/mL (0.12nM-12pM; Figure 2A). Next we evaluated whether the common Val34Leu polymorphism influences the detection of AP-FXIII. The results indicate that both variants are detected equally (Figure 2B). We performed further ELISA analyses to rule out any cross-reactivity with FXIII-deficient plasma, nonactivated normal plasma, and purified FXIII-A_2. No unspecific binding was detected, and we did not find any cross-reactivity of the monoclonal antibodies with FXIII-A_2 (data not shown), suggesting that the ELISA is selective for free AP-FXIII. In serum samples from 3 healthy donors we detected on average 313.3 ng/mL (41.5 ng/mL SD), corresponding approximately to the plasma concentration of FXIII tetramer.

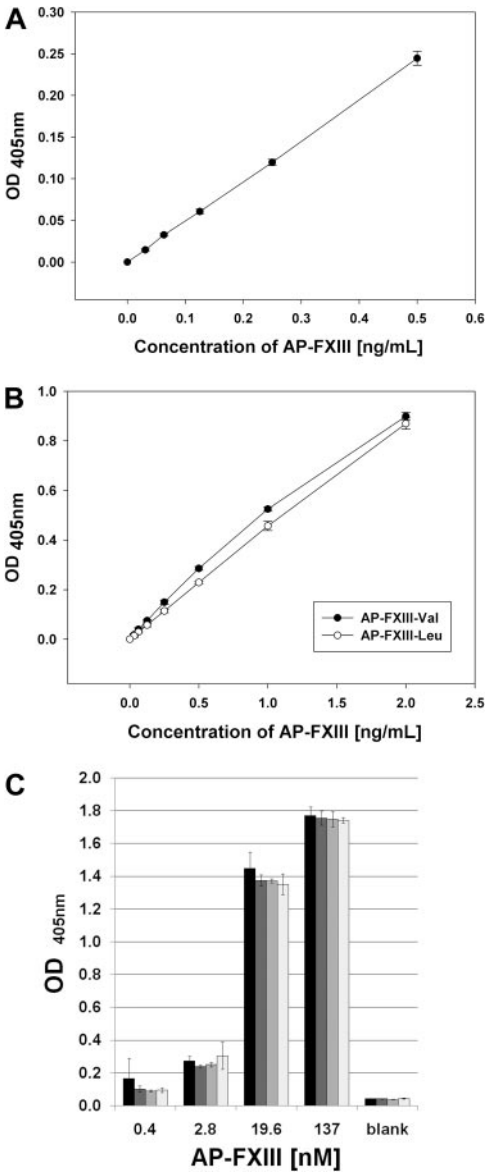

Figure 2. Characterization of the optimized AP-FXIII ELISA. (A) General sensitivity. Titration of synthetic AP-FXIII in dilution buffer at 0.5, 0.25, 0.125, 0.0625, and 0.03125 ng/mL (0.12 nM-7.8 pM). Mean values from quintuplicates with error bars representing SD are shown. (B) Evaluation of the sensitivity toward AP-FXIII-Val34Leu polymorphism. Synthetic AP-FXIII-Val (●) and AP-FXIII-Leu (○) were titrated at 2.0, 1.0, 0.5, 0.25, 0.125, 0.0625, and 0.03125 ng/mL (0.5 nM-7.8 pM). Mean values from triplicates with error bars representing SD are depicted. (C) Competition analysis for mAb-1286 and mAb-6B11. AP-FXIII was detected either by mAb-1286 only (■), or in a mixture with mAb-6B11 at 1 μg/mL (▩), 2 μg/mL (▨), or 4 μg/mL (□). Mean values of triplicates with error bars representing SD are depicted.

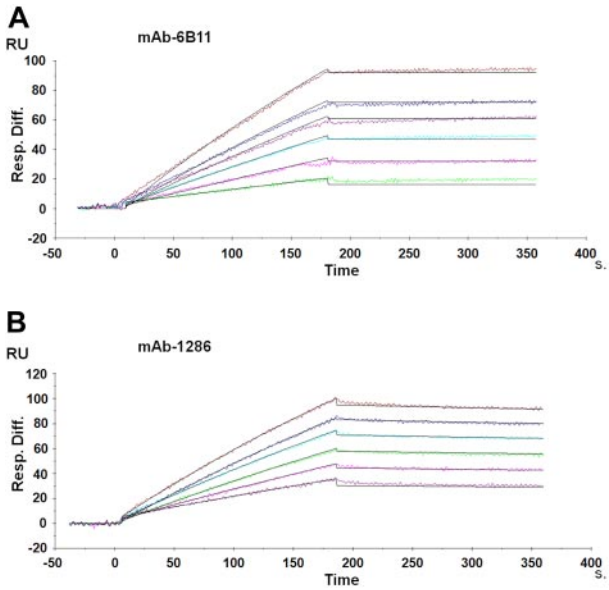

C

mAb	AP-FXIII	analysis	k_a[1/Ms]	k_d[1/s]	K_D[M]	average K_D[M]	range of variation of K_D[M]
6B11	Val	1st	$2.5x10^3$	$2.7x10^{-7}$	$1.1x10^{-10}$	**$5.5x10^{-11}$**	$1.1x10^{-10}$
		2nd	$1.2x10^5$	$5.3x10^{-8}$	$4.7x10^{-13}$		
	Leu	1st	$3.1x10^4$	$1.9x10^{-8}$	$6.1x10^{-13}$	**$2.6x10^{-12}$**	$3.9x10^{-12}$
		2nd	$5.3x10^4$	$2.4x10^{-7}$	$4.5x10^{-12}$		
1286	Val	1st	$2.0x10^5$	$3.4x10^{-4}$	$1.7x10^{-9}$	**$1.9x10^{-9}$**	$5.0x10^{-10}$
		2nd	$1.0x10^5$	$2.2x10^{-4}$	$2.2x10^{-9}$		
	Leu	1st	$2.3x10^5$	$3.5x10^{-4}$	$1.5x10^{-9}$	**$1.4x10^{-9}$**	$1.0x10^{-10}$
		2nd	$8.3x10^4$	$1.2x10^{-4}$	$1.4x10^{-9}$		

Figure 3. Binding affinity of anti-AP-FXIII monoclonal antibodies as measured by SPR. Sensorgrams of time (seconds) versus RUs are shown. (A) Binding of AP-FXIII-Val to mAb-6B11. The curves represent the association and dissociation rates of AP-FXIII-Val at the following concentrations: 2.5 (green), 5 (pink), 7.5 (cyan), 10 (magenta), 12 (dark blue), and 16nM (brown). (B) Binding of AP-FXIII-Val to mAb-1286 measured at the following concentrations: 5 (magenta), 7.5 (pink), 10 (green), 12.5 (cyan), 15 (dark blue), and 17.5nM brown). (C) Binding affinity data for mAb-6B11 and mAb-1286 and both AP-FXIII genotypes. The association rate constant k_a, the dissociation rate constant k_d and the equilibrium dissociation constant $K_{D\,=\,kd/ka}$ of 2 independent analyses (1st and 2nd) are shown, together with the average K_D and range of variation.

Analysis of the binding of both antibodies to free AP-FXIII

We used SPR to investigate the binding characteristics of mAb-6B11 and mAb-1286 to synthetic AP-FXIII-Val34 and AP-FXIII-Leu34. Either mAb-6B11 or mAb-1286 was immobilized onto the sensor chip surface, and binding curves were recorded for both AP-FXIII variants at 6 different concentrations between 17.5 and 2.5nM. Representative curves for AP-FXIII-Val binding to mAb-6B11 and to mAb-1286 are shown in Figure 3A and B.

Generally, the sensorgram curves for both antibodies with both AP-FXIII variants showed no significant dissociation phases. We also noticed this lack of dissociation during the regeneration of the chips under very stringent condition. The equilibrium dissociation constant K_D was calculated from the ratio of the measured kinetic

rate constants k_d/k_a. K_D values obtained for both antibodies with both AP-FXIII variants are shown in Figure 3C. We found greater binding affinities for mAb-6B11 compared with mAb-1286. The affinity did not differ significantly between the 2 AP-FXIII variants.

Binding site analysis of AP-FXIII by epitope mapping by the use of SPR

To localize the binding sites of mAb-6B11 and mAb-1286 on AP-FXIII we performed epitope mapping by using SPR and ELISA techniques. Figure 4A shows the amino acid sequences of AP-FXIII and the peptides used for epitope mapping. Peptides AP1-AP8 were 8 amino acids long and contained 4 overlapping residues. AP9 differed from AP8 by the Leu substitution at position 34. Additional peptides that were investigated for binding contained either the first 12 amino acids (AP1-12), or amino acids 3 to 12 (AP3-12), or the last 25 amino acids (AP13-37) of AP-FXIII.

In a first step, we measured binding of the short peptides to both antibodies. These short peptides were tested at a concentration of 10μM. Only the peptides AP1 (amino acids 1-8) and AP2 (amino acids 5-12) bound weakly to mAb-6B11 (Figure 4B). None of the short peptides showed any affinity toward mAb-1286 (data not shown). Next, we evaluated the affinity of mAb-6B11 toward the longer peptides AP1-12, AP3-12, and AP13-37. We measured a K_D of 2.0nM ($k_a = 1.5 \times 10^5$; $k_d = 3.1 \times 10^{-4}$) for AP1-12 and a K_D of 4.2nM ($k_a = 6.6 \times 10^4$; $k_d = 2.8 \times 10^{-4}$) for AP3-12. Figure 4C and D display the sensorgrams of AP1-12 and of AP3-12, from which the K_D for mAb-6B11 was calculated. No binding was observed with AP13-37, even at the greater concentration of 150nM (Figure 4E). Compared with full-length AP-FXIII (Table 3C) we measured lower affinities of mAb-6B11 toward the fragments AP1-12 and AP3-12. This difference in K_D indicates that both of these 2 peptides do not contain the whole epitope of mAb-6B11 because a similar K_D would be expected for a complete epitope. This finding suggests that mAb-6B11 binds to a conformational epitope that is formed mainly by amino acids within the first 12 amino acids. Although no binding of the fragment AP13-37 was observed, it could still contain amino acids that contribute to the formation of the complete epitope but are not sufficient for binding to mAb-6B11.

Subsequently, binding of the longer peptides AP1-12 and AP13-37 to mAb-1286 was tested. The sensorgrams revealed much weaker binding between mAb-1286 and AP13-37 compared with AP-FXIII and no interaction with AP1-12 (Figure 4F). Furthermore, the sensorgrams showed fast association and weak dissociation of AP-FXIII with mAb-1286.

Taken together, the results imply that both antibodies recognize conformational epitopes that do not overlap.

Epitope mapping of AP-FXIII by ELISA

To confirm the SPR results, we also performed epitope mapping by ELISA. The same peptides as described previously were directly coated onto microtiter plates and analyzed for binding to mAb-6B11 and mAb-1286. Table 1 summarizes the results from the ELISA tests. The antibody mAb-6B11 only recognized AP1 and AP2 of the 9 short peptides. The longer peptides AP1-12 and AP3-12 resulted in greater OD signals compared with the signal obtained for AP2. No binding at all could be detected to AP13-37.

For mAb-1286, we observed no significant binding to AP1-12, weak binding to peptide AP7, and strong binding to AP13-37 (Table 1). In addition, we performed this ELISA experiment with a dilution range from 1.6μM to 0.1nM and compared OD values for

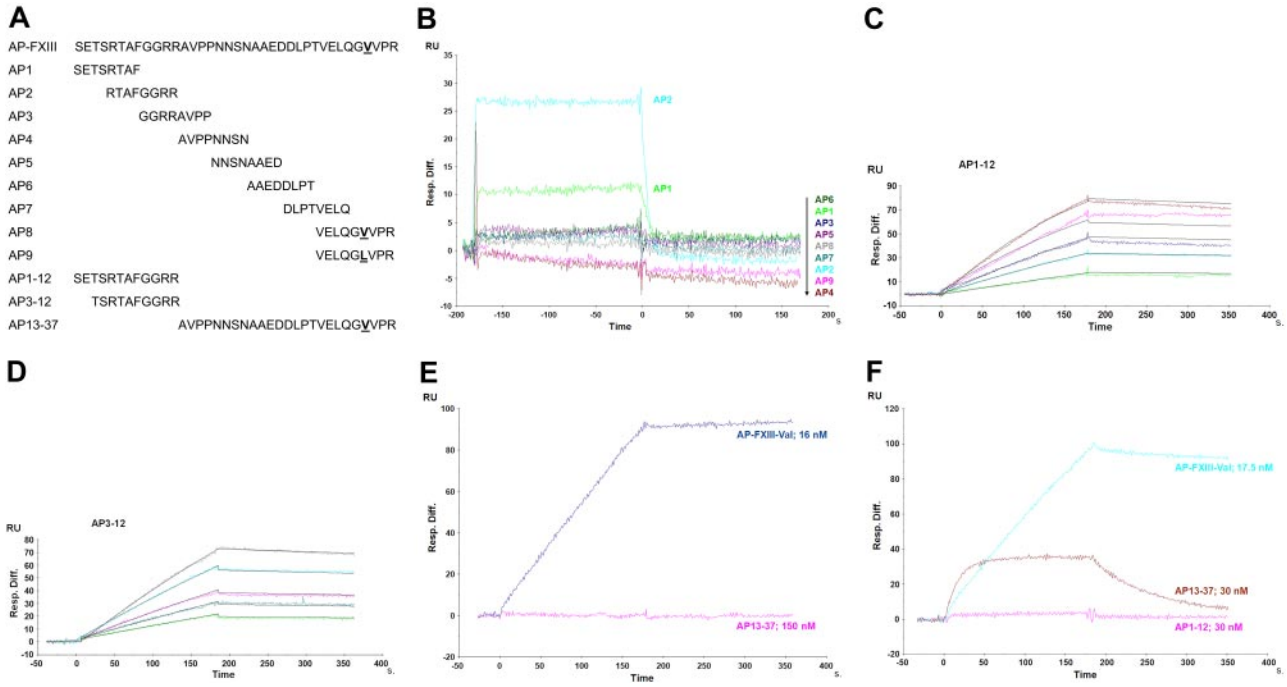

Figure 4. Epitope mapping with SPR showing sensorgrams of time (seconds) versus RU. (A) Sequences of peptides analyzed for epitope mapping of mAb-6B11 and mAb-1286. Amino acid sequences of full-length AP-FXIII and all overlapping peptides used for the epitope mapping are depicted. AP8 and AP9 differ in residue 34 containing either a Val or Leu, respectively. (B) Epitope mapping of mAb-6B11. Peptides AP1-AP9 were tested for binding to mAb-6B11 at a concentration of 10μM. All peptides are listed downward corresponding to their colored curves. (C-D) Affinity analysis of mAb-6B11 to AP1-12 and AP3-12. The affinity of mAb-6B11 to AP1-12 was measured at the following concentrations: 5 (green), 10 (cyan), 15 (dark blue), 20 (pink), and 30nM (brown) and to AP3-12 at the concentrations: 5 (green), 7.5 (aquamarine), 10 (pink), 15 (cyan), and 20nM (gray). (E) Localization of the binding site of mAb-6B11. mAb-6B11 was tested for binding to AP-FXIII-Val at a concentration of 16nM (purple) and AP13-37 at 150nM (pink). (F) Localization of the binding site of mAb-1286. The following peptides were tested for binding: AP-FXIII-Val at a concentration of 17.5nM (cyan), and AP13-37 (brown), and AP1-12 at 30nM (pink).

Table 1. Epitope mapping by ELISA

Peptide	OD 405 nm
mAB-6B11	
Full-length AP-FXIII (1-37)	> 3.000
AP1	0.054
AP2	1.712
AP1-12	2.625
AP3-12	2.563
AP13-37	0.038
Blank	0.039
mAb-1286	
Full-length AP-FXIII (1-37)	> 3.000
AP1-12	0.081
AP3-12	0.121
AP7	0.849
AP13-37	> 3.000
Blank	0.045

Peptides were tested at concentrations of 40μM and mean OD values of duplicates are shown.

ELISA indicates enzyme-linked immunosorbent assay; and OD, optical density.

AP13-37 with full-length AP-FXIII. The results suggest that AP13-37 binds to mAb-1286 over a wide concentration range and even at very low concentrations (data not shown). This finding supports the conclusion of high-affinity binding of this C-terminal fragment. Compared with full-length AP-FXIII, however, the binding affinity was weaker, which may indicate that amino acids in the C-terminal part are crucial for the formation of a conformational epitope.

In addition, we verified that mAb-6B11 and mAb-1286 do not compete with each other for binding to AP-FXIII. As shown in Figure 2C, there were no significant differences in detection of AP-FXIII by mAb-1286 in absence or presence of mAb-6B11. These results are further evidence that the binding sites of mAb-6B11 and mAb-1286 do not overlap. Taken together, the results from the epitope mapping analysis by ELISA were in agreement with the data obtained from our SPR studies.

Analysis of AP-FXIII by NMR

We have determined conformational preferences of recombinant AP-FXIII in plain water as well as in plasma. The stability of the AP-FXIII in plasma, however, was insufficient unless the temperature was lowered to 4°C, where reproducible spectra could be recorded over a time range of 3 days. NMR experiments were conducted at pH 5.5 (both in water and in plasma) to reduce unfavorable amide proton exchange at greater pH that resulted in broad lines.[16] In addition circular dichroism spectra were recorded at physiologic pH 7.0 and the lower pH 5.5. The data indicate that neither α-helical nor β-strand type secondary structural elements become populated at the greater pH value, although slightly more polyproline-type absorption at 208 nm occurs at the greater pH value (data not shown). The [^{15}N,^{1}H]-HSQC spectra of the AP-FXIII in water revealed the presence of too many peaks, and the extra peaks were attributed to the presence of *cis* conformers about the Pro-peptide bonds. The presence of these additional peaks already indicated that AP-FXIII in water was mainly unstructured. The backbone of the AP-FXIII in solution could be fully assigned in water and to 60% in plasma. We attribute the lower percentage of assignments to the line-broadening at the lower temperature and the increased viscosity of the plasma solution.

To thoroughly investigate whether the AP-FXIII is partially folded, we decided to use ^{15}N relaxation NMR experiments. The required ^{15}N-labeled AP-FXIII was produced in milligrams per liter quantities in *E coli* biosynthetically from ubiquitin fusion peptides. To assess whether segments of the polypeptide chain are folded, a ^{15}N{^{1}H}-NOE experiment was recorded. Typically, amide nitrogen atoms of well-structured regions adopt values larger than 0.5, whereas for fully flexible regions the values are negative. In our experience secondary structure can only be reliably determined by NMR if the H-NOE in the corresponding segment is larger than 0.4. Values of the ^{15}N{^{1}H}-NOE of AP-FXIII are depicted in Figure 5 for both environments. Clearly, no values larger than 0.4 are encountered, and for many residues the heteronuclear NOE is close to 0.2, indicating that they are not fully flexible but that structure determination using NMR is not possible. Therefore, no in-depth structural studies were performed.

Discussion

We have previously reported that AP-FXIII is released from the FXIII A-subunit upon thrombin cleavage and that free AP-FXIII possibly assumes a different conformation compared with its bound form.[7] The objective of this study was to characterize free AP-FXIII by 2 novel approaches, which include binding studies with specific monoclonal antibodies and NMR.

Within the nonactivated FXIII A-subunit dimer, AP-FXIII is located on the surface of the molecule, and this exposed position may promote the release of the AP-FXIII from the molecule into plasma upon activation. A loop containing the thrombin cleavage site Arg37-Gly38 protrudes from the molecule, making this site accessible to the protease. The Leu variant of the Val34Leu polymorphism has been shown to favor the interaction with thrombin leading to improved activation kinetics.[20] The loop as well as the 4 N-terminal amino acids are flexible and hence not resolved in the crystal structure. Otherwise, the AP-FXIII assumes a defined conformation within the FXIII A-subunit dimer. Close interactions with the molecular environment, in particular 17 H-bonds between the amino acids of the AP-FXIII and amino acids of its own monomer as well as with the other monomer may be crucial to maintain the structure and position of the AP-FXIII within the molecule.

This defined conformation must be altered or lost in free AP-FXIII because it can be selectively detected by the use of the optimized AP-FXIII ELISA without any cross-reactivity with zymogen FXIII-A_2B_2 present in normal plasma or other plasma components in FXIII-deficient plasma. We therefore conclude that the 2 monoclonal antibodies mAb-6B11 and mAb-1286 are specific

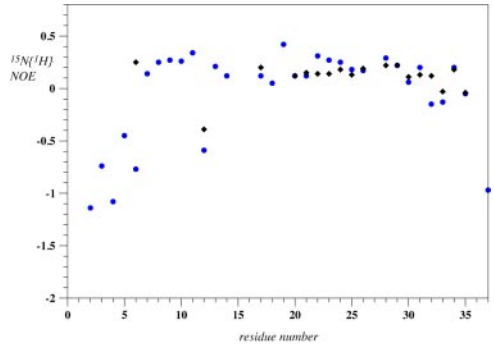

Figure 5. ^{15}N{^{1}H}-NOE values of recombinant AP-FXIII in plain aqueous buffer (blue circles) as well as in plasma (black diamonds) at pH 5.5. No values are presented in plasma for residues 2 to 5, 7 to 11, 13, 14, 18, 19, 36, and 37 because those signals could not be assigned.

for free AP-FXIII. The optimized ELISA also proved sensitive to detect AP-FXIII at a concentration as low as 12pM. Measurements in serum confirmed that the ELISA is able to detect native AP-FXIII.

We further investigated whether the common Val34Leu polymorphism influences the detection of the free AP-FXIII. Both antibodies mAb-6B11 and mAb-1286 bound equally well to both AP-FXIII variants, and binding affinities were not affected by the Val34Leu polymorphism. Therefore, the described protective effect of the Val34Leu polymorphism against myocardial infarction, deep venous thrombosis, and ischemic stroke[4,21-27] is most likely only mediated by structural characteristics of the bound AP-FXIII, which influence the affinity of thrombin to the bound AP-FXIII.

Epitope mapping analyses suggested that the antibody mAb-6B11 binds to the N-terminal region of AP-FXIII (amino acids 1-12), whereas the antibody mAb-1286 recognizes the C-terminal region (amino acids 13-37), and hence the 2 antibodies do not compete for binding.

For the first time, we conducted a structural analysis of recombinant AP-FXIII using solution NMR techniques. These experiments indicated a high conformational flexibility of the peptide in both water and plasma environments, precluding a more detailed structural characterization by NMR. However, the relaxation data of the peptide in water revealed no experimental evidence for the presence of a short hairpin, which we previously proposed on the basis of molecular modeling.[7] The finding that the released peptide is unstructured, as demonstrated by the NMR studies, suggests that binding to the monoclonal antibodies proceeds in an induced-fit mode.[28] Thus, the specificity of the antibodies for free AP-FXIII may be explained as follows: the rigid form of the AP-FXIII bound to FXIII zymogen is incompatible with this antibody binding mode and/or residues crucial for antibody recognition are buried within the protein and hence inaccessible to the antibodies.

In summary, our study confirms that released AP-FXIII can be distinguished from AP-FXIII bound to zymogen FXIII and can be detected with a specific and sensitive ELISA. We hypothesize that detection of AP-FXIII might represent a new diagnostic marker for acute thrombotic events because the presence of this peptide in plasma reflects the earlier stage of coagulation. This is in contrast to the measurement of D-dimer levels, a widely used diagnostic tool for venous thromboembolism,[29] pulmonary embolism,[30,31] and stroke.[32,33] D-dimers are clot degradation products and reflect thrombotic events retrospectively, and their absence is mainly used to exclude thrombosis. The detection of AP-FXIII might therefore complement diagnostic strategies for accurate diagnosis of acute thrombotic events. We also showed that the common Val34Leu polymorphism does not influence the detection of free AP-FXIII with respect to affinity and sensitivity toward the antibodies. This finding presents an important issue because the polymorphism has a high allele frequency in the white population and could prevent a possible diagnostic application of the detection of released AP-FXIII. Although the proof-of-principle has been shown in this article, clinical studies in patients who experience acute myocardial infarction, stroke, or venous thromboembolism are needed to assess the suitability of released AP-FXIII as a marker for acute thrombotic events.

Acknowledgments

We thank Dr Monique Vogel and Alexander Eggel (Institute of Immunology, University of Bern) for technical assistance with the BiacoreX.

This work was funded by grants from the Swiss National Science Foundation (grant no. 32003B-116262), the Stanley Thomas Johnson Foundation, and OPO Foundation.

Authorship

Contribution: E.O. designed the project, performed ELISA and SPR experiments, analyzed the data, and wrote the paper; V.S. designed the project, performed the structural analysis using the Swiss PDB Viewer, constructed and expressed ^{15}N-labeled peptides for NMR analysis, and wrote the paper; R.W. designed, performed and analyzed the NMR studies; O.Z. designed and analyzed the NMR studies and wrote the paper; and H.P.K. designed the project, analyzed the data, and wrote the paper.

Conflict-of-interest disclosure: The authors declare no competing financial interests.

Correspondence: Prof Hans-Peter Kohler, MD, Department of Hematology, Hemostasis Research Laboratory, Ludwig Haus, University Hospital Bern, Inselspital, 3010 Bern, Switzerland; e-mail: hanspeter.kohler@spitalnetzbern.ch.

References

1. Muszbek L, Bagoly Z, Bereczky Z, Katona E. The involvement of blood coagulation factor XIII in fibrinolysis and thrombosis. *Cardiovasc Hematol Agents Med Chem.* 2008;6(3):190-205.
2. Kohler HP. Role of blood coagulation factor XIII in vascular diseases. *Swiss Med Wkly.* 2001;131(3-4):31-34.
3. Kohler HP, Mansfield MW, Clark PS, Grant PJ. Interaction between insulin resistance and factor XIII Val34Leu in patients with coronary artery disease. *Thromb Haemost.* 1999;82(3):1202-1203.
4. Kohler HP, Stickland MH, Ossei-Gerning N, Carter A, Mikkola H, Grant PJ. Association of a common polymorphism in the factor XIII gene with myocardial infarction. *Thromb Haemost.* 1998;79(1):8-13.
5. Kucher N, Schroeder V, Kohler HP. Role of blood coagulation factor XIII in patients with acute pulmonary embolism. Correlation of factor XIII antigen levels with pulmonary occlusion rate, fibrinogen, D-dimer, and clot firmness. *Thromb Haemost.* 2003;90(3):434-438.
6. Montaner J, Perea-Gainza M, Delgado P, et al. Etiologic diagnosis of ischemic stroke subtypes with plasma biomarkers. *Stroke.* 2008;39(8):2280-2287.
7. Schroeder V, Vuissoz JM, Caflisch A, Kohler HP. Factor XIII activation peptide is released into plasma upon cleavage by thrombin and shows a different structure compared with its bound form. *Thromb Haemost.* 2007;97(6):890-898.
8. Yee VC, Pedersen LC, Le Trong I, Bishop PD, Stenkamp RE, Teller DC. Three-dimensional structure of a transglutaminase: human blood coagulation factor XIII. *Proc Natl Acad Sci U S A.* 1994;91(15):7296-7300.
9. Yee VC, Pedersen LC, Bishop PD, Stenkamp RE, Teller DC. Structural evidence that the activation peptide is not released upon thrombin cleavage of factor XIII. *Thromb Res.* 1995;78(5):389-397.
10. Weiss MS, Metzner HJ, Hilgenfeld R. Two nonproline cis peptide bonds may be important for factor XIII function. *FEBS Lett.* 1998;423(3):291-296.
11. Guex N, Peitsch MC. SWISS-MODEL and the Swiss-PdbViewer: an environment for comparative protein modeling. *Electrophoresis.* 1997;18(15):2714-2723.
12. Nice EC, Catimel B. Instrumental biosensors: new perspectives for the analysis of biomolecular interactions. *Bioessays.* 1999;21(4):339-352.
13. Kohno T, Kusunoki H, Sato K, Wakamatsu K. A new general method for the biosynthesis of stable isotope-enriched peptides using a decahistidine-tagged ubiquitin fusion system: an application to the production of mastoparan-X uniformly enriched with 15N and 15N/13C. *J Biomol NMR.* 1998;12(1):109-121.
14. Miroux B, Walker JE. Over-production of proteins in *Escherichia coli*: mutant hosts that allow synthesis of some membrane proteins and globular proteins at high levels. *J Mol Biol.* 1996;260(3):289-298.
15. Cavangh J, Fairbrother WJ, Palmer AG, Skelton NJ. *Protein NMR Spectroscopy: Principles and Practice.* San Diego, CA: Academic Press; 1996.

16. Wüthrich K. *NMR of Proteins and Nucleic Acids*. 1st ed. New York, NY: John Wiley & Sons; 1986.
17. Noggle JH, Schirmer RE. *The Nuclear Overhauser Effect–Chemical Applications*. New York, NY: Academic Press; 1971.
18. Bartels C, Billeter M, Güntert P, Wüthrich K. The program XEASY for computer-supported NMR spectral analysis of biological macromolecules. *J Biomol NMR*. 1995;6(1):1-10.
19. Keller R. *The Computer Aided Resonance Assignment*. Goldau, Switzerland: Cantina Verlag; 2004.
20. Trumbo TA, Maurer MC. Thrombin hydrolysis of V29F and V34L mutants of factor XIII (28-41) reveals roles of the P(9) and P(4) positions in factor XIII activation. *Biochemistry*. 2002;41(8):2859-2868.
21. Catto AJ, Kohler HP, Coore J, Mansfield MW, Stickland MH, Grant PJ. Association of a common polymorphism in the factor XIII gene with venous thrombosis. *Blood*. 1999;93(3):906-908.
22. Franco RF, Pazin-Filho A, Tavella MH, Simoes MV, Marin-Neto JA, Zago MA. Factor XIII Val34Leu and the risk of myocardial infarction. *Haematologica*. 2000;85(1):67-71.
23. Franco RF, Reitsma PH, Lourenco D, et al. Factor XIII Val34Leu is a genetic factor involved in the etiology of venous thrombosis. *Thromb Haemost*. 1999;81(5):676-679.
24. Wartiovaara U, Perola M, Mikkola H, et al. Association of FXIII Val34Leu with decreased risk of myocardial infarction in Finnish males. *Atherosclerosis*. 1999;142(2):295-300.
25. Shafey M, Anderson JL, Scarvelis D, Doucette SP, Gagnon F, Wells PS. Factor XIII Val34Leu variant and the risk of myocardial infarction: a meta-analysis. *Thromb Haemost*. 2007;97(4):635-641.
26. Wells PS, Anderson JL, Scarvelis DK, Doucette SP, Gagnon F. Factor XIII Val34Leu variant is protective against venous thromboembolism: a HuGE review and meta-analysis. *Am J Epidemiol*. 2006;164(2):101-109.
27. Vokó Z, Bereczky Z, Katona E, Adany R, Muszbek L. Factor XIII Val34Leu variant protects against coronary artery disease. A meta-analysis. *Thromb Haemost*. 2007;97(3):458-463.
28. Koshland DE. Application of a theory of enzyme specificity to protein synthesis. *Proc Natl Acad Sci U S A*. 1958;44(2):98-104.
29. Geersing GJ, Janssen KJ, Oudega R, et al. Excluding venous thromboembolism using point of care D-dimer tests in outpatients: a diagnostic meta-analysis. *Br Med J*. 2009;339:b2990.
30. Karami-Djurabi R, Klok FA, Kooiman J, Velthuis SI, Nijkeuter M, Huisman MV. D-dimer testing in patients with suspected pulmonary embolism and impaired renal function. *Am J Med*. 2009;122(11):1050-1053.
31. Lobo JL, Zorrilla V, Aizpuru F, et al. D-dimer levels and 15-day outcome in acute pulmonary embolism. Findings from the RIETE registry. *J Thromb Haemost*. 2009;7(11):1795-1801.
32. Koch HJ, Horn M, Bogdahn U, Ickenstein GW. The relationship between plasma D-dimer concentrations and acute ischemic stroke subtypes. *J Stroke Cerebrovasc Dis*. 2005;14(2):75-79.
33. Skoloudik D, Bar M, Sanak D, et al. D-dimers increase in acute ischemic stroke patients with the large artery occlusion, but do not depend on the time of artery recanalization. *J Thromb Thrombolysis*. 2010;29(4):477-482.